EPTT-2024- 0022
DYNAMICS OF H_2 BUBBLES BASED ON VELOCITY FIELDS DURING WATER ELECTROLYSIS

Jeferson Diehl de Oliveira[1]
[1]SISEA - Renewable and Alternative Energy Systems Laboratory, Polytechnic School of the University of São Paulo, São Paulo, Brazil
jef.diehl@usp.br

Clauber André Ferasso[2]
[2]PPGE3M - Postgraduate in Mining, Metallurgical and Materials Engineering, Federal University of Rio Grande do Sul, Porto Alegre, Rio Grande do Sul, Brazil
clauber.ferasso@fsg.edu.br

Elaine Maria Cardoso[3]
[3]UNESP - São Paulo State University, School of Engineering, São João da Boa Vista, SP, Brazil
elaine.cardoso@unesp.br

Lina Maria Varón[1]
[1]SISEA - Renewable and Alternative Energy Systems Laboratory, Polytechnic School of the University of São Paulo, São Paulo, Brazil
varon@usp.br

Jacqueline Baincon Copetti[4]
[4]LETEF, Laboratory of Thermal and Fluid Dynamic Studies, University of Vale do Rio dos Sinos, São Leopoldo, RS, Brazil
jcopetti@unisinos.br

Abstract. *This research examines the electrolysis process using nickel-iron electrodes immersed in two types of electrolytes: one consisting of 30% KOH alone and another with 30% KOH supplemented by 2.5 g of ionic liquid (BMI.BF4). The electrodes were spaced 40 mm apart, and 55, 110, and 165 A/m^2 current densities were applied. The study involved capturing and analyzing images of hydrogen evolution to investigate the impact of the ionic liquid on ionic conductivity. Findings, illustrated through images showing vertical velocity, vorticity, and velocity field, suggest potential enhancements in hydrogen generation, characterized by larger bubble volumes and improved vertical displacement speeds of bubbles when the ionic liquid is introduced into the electrolyte.*

Keywords: *Electrolytic process, Ionic solution, Visual motion analysis, Hydrogen generation*

1. INTRODUCTION

In recent years, energy generation and transformation have become critical issues, primarily due to their environmental repercussions. This rising concern has emphasized the necessity for developing cleaner and more sustainable energy sources. Consequently, green hydrogen, produced via electrolysis, has become an attractive solution because of its low environmental impact and high energy content (Nasser et al., 2022; Chien et al., 2021). Despite its potential, significant challenges still exist in increasing hydrogen production efficiency through electrolysis (Nasser et al., 2022). The flow field of electrolytes is crucial in controlling ionic mass transfer, temperature distribution, bubble sizes, bubble detachment, and rising velocity. These elements significantly affect current and potential distributions within the electrolysis reactor. Such a phenomenon is a complex topic that remains incompletely understood, necessitating further research.

Avci and Toklu (2022) explored the flow dynamics of bubbles in water electrolysis with vertical electrodes. They examined how the void fraction, which is the space between the electrodes, affects bubble size and speed. Their research led to the creation of a formula to estimate the acceleration velocity of hydrogen gas post-production. Additionally, they found that the velocity of hydrogen gas bubbles separating from the electrode is influenced not only by drag and buoyancy forces but also by the drift coefficient.

Park et al. (2022) examined the impact of hydrodynamic parameters on critical current density, focusing on factors such as void fraction and mass flux during electrolysis. The findings indicated that an increase in mass flux delayed the formation of the film, thereby raising the critical current density, regardless of the channel's angle or the inlet void fraction. Additionally, a higher void fraction resulted in varying flow patterns, shifting from dispersed bubbles to slug flow, based on parameters like inlet void fraction and electrode tilt.

Convection can be driven by natural buoyancy or forced methods, while diffusion is caused by concentration gradients of reactants and products at the electrode-electrolyte interface and throughout the bulk. Consequently, significant research has focused on the dynamic fluid behavior of the gas phase, including the impacts of convection, velocity profiles, bubble initiation, and the effects of factors such as current density, electrode spacing, concentration, temperature, and pressure. Numerous studies have explored various aspects of water electrolysis, with a particular emphasis on the fluid dynamic properties of bubbles. To investigate these aspects, a range of experimental techniques have been used to visualize velocity fields and bubble growth, including Particle Image Velocimetry (PIV), Laser Doppler Velocimetry (LDV), Planar Laser-Induced Fluorescence (PLIF), and Particle Tracking Velocimetry (PTV) (Chandran et al., 2015; Jianu et al., 2015; Zhu et al., 2018; Babu and Das, 2019; Li et al., 2021; Oliveira et al., 2024).

Despite numerous studies on hydrogen generation and transport during electrolysis, understanding bubble dynamics in this process remains challenging. One major difficulty lies in comprehending the two-phase flow dynamics within the electrolyte, driven by convection and vorticity zones generated by turbulence. Consequently, this study aims to analyze velocity fields during alkaline water electrolysis using an optical flow method, considering the effects of current density and electrode gap.

2. METHODOLOGY

In order to perform the experiment of generating hydrogen via water electrolysis, a polylactic acid (PLA) support was fabricated using a 3D printer to secure the Ni-Fe electrodes. The casing was removed for this phase, and the electrolyte was poured into the previously described glass container. A direct current (DC) power source was utilized to supply electrical current to the electrodes. To capture and identify hydrogen production, images were captured using a high-speed camera MotionPro model Y4-S1, using 600 frames per second (Δt = 1.67 s), with a pixel size Δh of 37.5 μm. The experimental setup comprises a testing section housing a cubic container (the electrolyzer) with a volume of 600 ml, along with a DC power supply unit, specifically the Minipa MPL-3305 model. The vertical working electrodes are constructed from Ni and Fe, chosen for their stability in an alkaline environment. The electrodes, each measuring 75 mm in width and 90 mm in length, were positioned vertically, maintaining a 20 mm separation between them, as shown in Figure 1. The experiment was conducted under ambient conditions, approximately 23 °C, utilizing an aqueous solution of potassium hydroxide (KOH) at a concentration of 30% relative to deionized water. This solution was contained within a glass vessel (the electrolyzer) measuring 100 mm × 12 mm × 90 mm. The experiments were repeated by adding 2.5 g of ionic liquid (IL) BMI.BF4 to the electrolyte, creating a mixture. Different current densities were applied, specifically 55, 110, and 165 A/m^2, accompanied by voltages varying between 3 and 8 V. These voltage values were contingent upon the concentration of the IL present in the solution. The selection of weight was guided by references (Souza et al., 2003; Dupont et al., 2006; Loget et al, 2009; Souza et al., 2009; Abdelouahed et al., 2014; Borba et al., 2017; Trombetta et al., 2019; Chen et al., 2022), which provided insight into the author's prior work on utilizing the ionic liquid (IL) in capacitors. The IL was chosen to have a molar fraction between 0.20 and 0.40 and demonstrated a conductivity (σ) exceeding 15 mS/cm at a temperature of 20 °C.

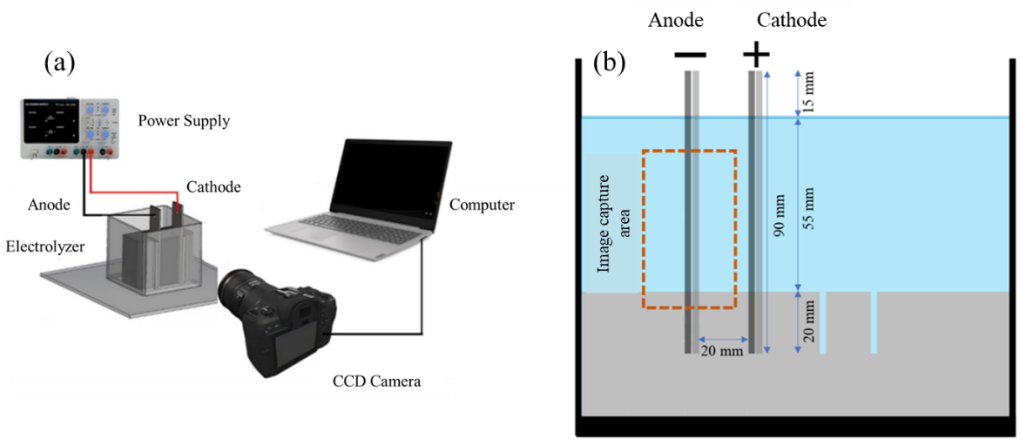

Figure 1. (a) Experimental setup; (b) Representative diagram of the hydrogen generation experiment.

2.1 Optical Flow

Optical flow techniques provide numerous benefits across various applications, and recent years have seen substantial progress in this area, as evidenced by several studies (Sun *et al*. 2014; Zhang *et al*. 2017; Li *et al*. 2017; Mei *et al*. 2019; Zhen *et al*. 2020). These methods are particularly effective for tracking and motion analysis, allowing for the detection and segmentation of objects based on their consistent movement patterns. Optical flow can function in real-time, making it well-suited for tasks that require fast video analysis, such as monitoring bubble generation. Its versatility and usefulness make optical flow an essential tool in computer vision, facilitating the analysis and interpretation of dynamic visual data. In this study, the optical flow method used is based on the approach developed by Liu and Shen (2008). This approach tackles the optical flow equation for diverse flow visualizations expressed in terms of image coordinates.

$$\frac{\partial g}{\partial f} + \nabla \cdot (g\boldsymbol{u}) - f(x, y, g) = \ 0 \tag{1}$$

where g represents the normalized image intensity, which is directly related to the radiance captured by the camera. The velocity in the image plane, denoted as $\boldsymbol{u} = (\boldsymbol{u_x}, \boldsymbol{u_y})$, is referred to as the optical flow. The operator $\nabla \equiv \partial/\partial x_i$ signifies the spatial gradient, while $f(x, y, g)$ denotes a boundary and diffusion term. Optical flow does not exhibit divergence-free characteristics, meaning $\nabla \cdot \boldsymbol{u} \neq 0$. However, under conditions where $f(x, y, g) = 0$ and $g\nabla \cdot \boldsymbol{u} = 0$, Eq. (1) simplifies to the Horn-Schunck brightness constraint equation $\partial g/\partial t + \mathbf{u}\cdot\nabla g = 0$. The analysis of optical flow data was carried out using MATLAB™, employing the open-source code provided by Horn et al. (1981), designed to compute the instantaneous velocity field from consecutive pairs of images.

To determine the optical flow, a variational formulation with a smoothness constraint is used, based on the functional described in Eq. (2).

$$j(\boldsymbol{u}) = \int_{\Omega} \left\{ \left[\frac{\partial g}{\partial t} + \nabla \cdot \left(g\vec{U} \right) \right]^2 + \lambda \left(|\nabla u_x|^2 + \left|\nabla u_y\right|^2 \right) \right\} dxdy \tag{2}$$

where λ represents the Lagrange multiplier, and Ω denotes the image domain. By minimizing Eq. (2), the Euler-Lagrange equations are derived as follows:

$$g\nabla \left[\frac{\partial g}{\partial t} + \nabla \cdot \left(g\vec{U} \right) - f \right] + \lambda \nabla^2 \boldsymbol{u} = 0 \tag{3}$$

The solution to Eq. (3) is obtained using the standard finite difference method with a Neumann boundary condition, where $\partial \vec{U}/\partial n = 0$ on the image domain.

3. RESULTS

During electrolysis, various bubble distributions arise due to fluid dynamics, as depicted in Fig. 2(a) for J = 55 A/m². Small bubbles dispersed away from the cathode guided by buoyancy and electrolyte dynamics **(1)**; curtains of bubbles generated along the electrode surface with predominantly vertical velocity and horizontal fluctuations during ascent **(2)**; larger bubbles tend to remain in certain positions for extended periods, inhibiting the activation of new nucleation sites **(3)**. Larger bubbles tend to form in deeper electrode regions and are released along with the bubble curtain, exhibiting higher velocities due to their volume **(4)**. These patterns display fluctuations over time and throughout the electrolyte owing to the turbulent characteristics of bubble dynamics. Figure 2(b) displays the height levels studied to evaluate the vertical velocity profile. The 0 mm level, in this case, represents half the height of the submerged electrode. The influence of current density on H_2 bubble generation and its dynamic (Vogt, 2013) is exemplified in Fig. 3 for 30% KOH and Fig. 4 for 30% KOH with IL diluted in electrolyte. In both cases, the dispersion of bubbles is evident, with both hydrogen bubbles predominantly released through dispersed bubbles forming along the cathode. The dispersion of bubbles in the electrolyte increases with the rise in current density. Under temporarily static conditions, larger bubbles can also be observed adhering to the cathode wall. These bubbles form as smaller bubbles coalesce at distinct nucleation sites. As the current density increases, a higher concentration of bubbles near the electrolyte's surface is observed. Figure 4 depicts H_2 bubbles with smaller diameters and a thinner bubble curtain. Indeed, the use of IL enhances the conductivity of the electrolyte medium, resulting in a decrease in both bubble growth and departure times. In this scenario, larger bubbles attached to the cathode wall are not observed.

3.1 Effect of current density on the velocity field

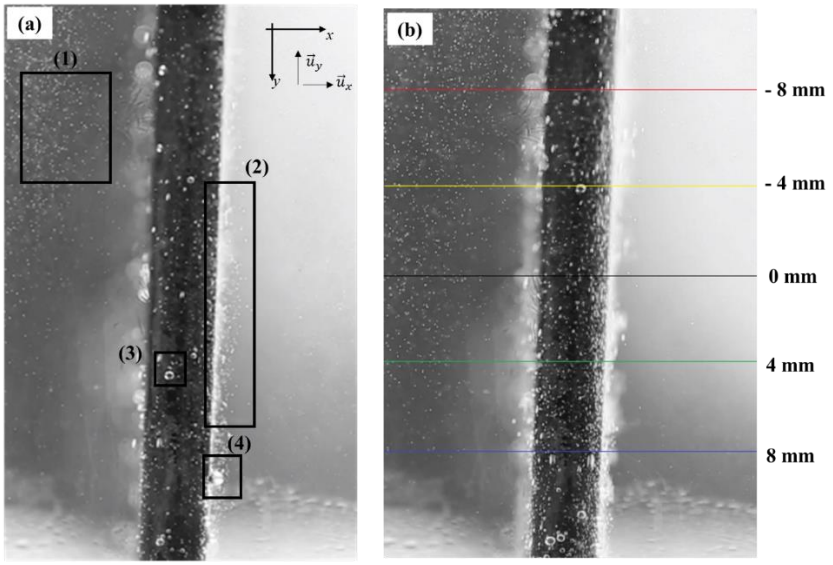

Figure 2. (a) Characteristic H_2 bubble distribution for J = 55 A/m² and 30% KOH; (b) height levels considered in this study to investigate u_y velocity.

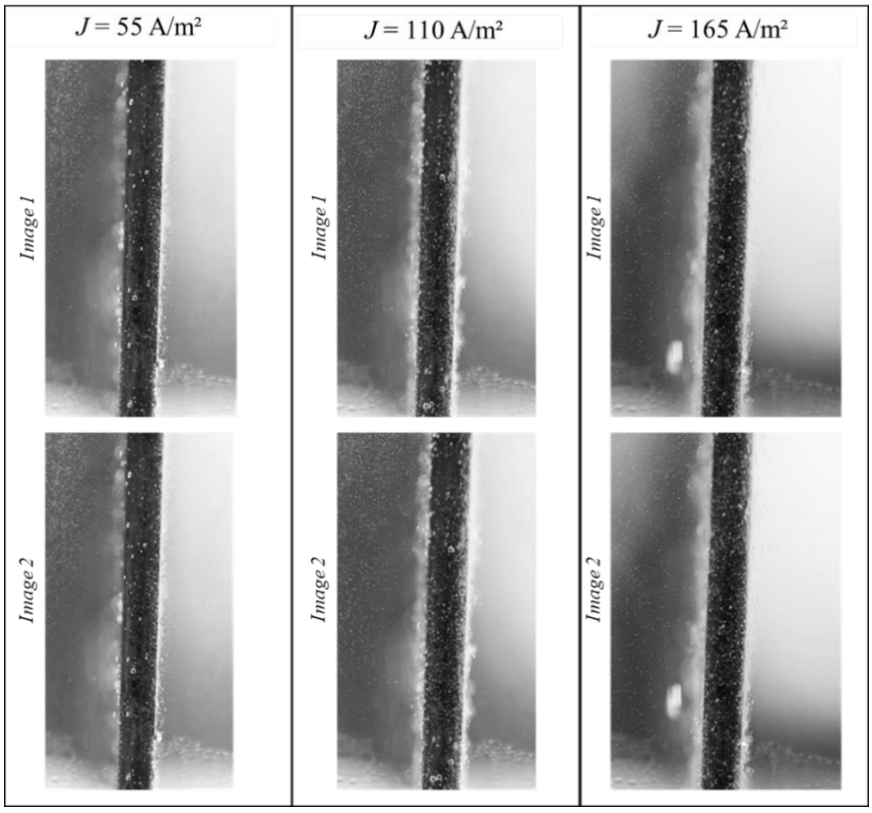

Figure 3. Sample of a pair of images with 30% KOH showing the presence of H_2 bubbles around the electrode for different current densities.

The velocity field between the electrodes was derived by sequentially analyzing pairs of images through the optical flow method. Figure 5 illustrates samples of the velocity fields obtained for 30% KOH as a function of current density. As anticipated, the augmentation in velocity field intensity correlates with the rise in current density, showcasing erratic behaviors linked to heightened electrolyte turbulence. For J = 55 A/m², the velocity field predominantly exhibits a vertical pattern, although the velocity field exhibits greater intensity on the right side of the electrode; this is attributed to the higher production of H_2 resulting from lower electrical resistance. As current density increases, nucleation sites increase, leading to greater uniformity in H_2 formation on both electrode sides and in higher bubble velocity. Consequently, velocity

fluctuations are observed along both the vertical and horizontal directions. Figure 6 presents the velocity field for 30% KOH+IL considering the same current densities. As it can be seen, the vertical velocity increases with the presence of IL.

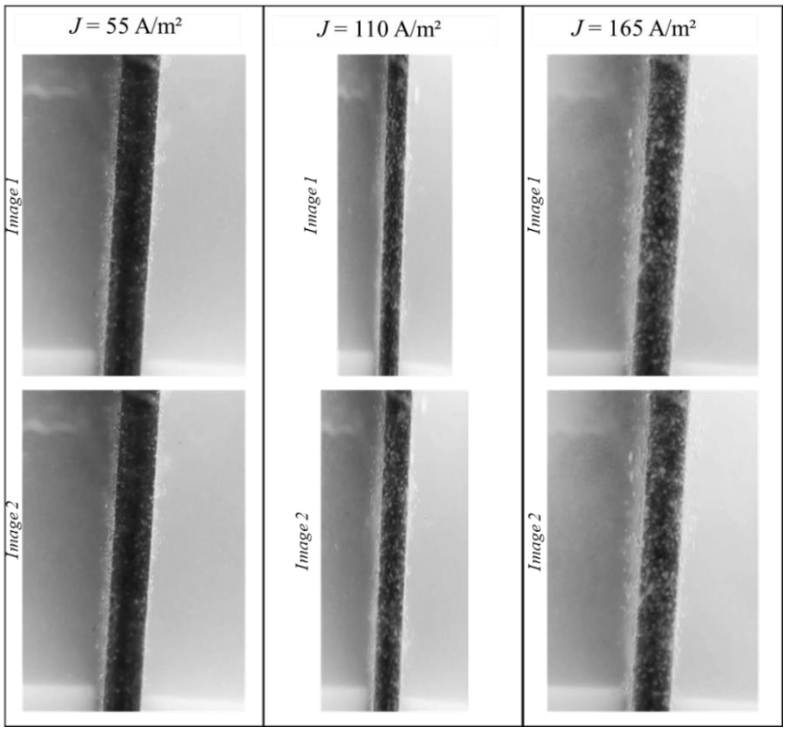

Figure 4. Sample of a pair of images with 30% KOH with IL showing the presence of H_2 bubbles for different current densities.

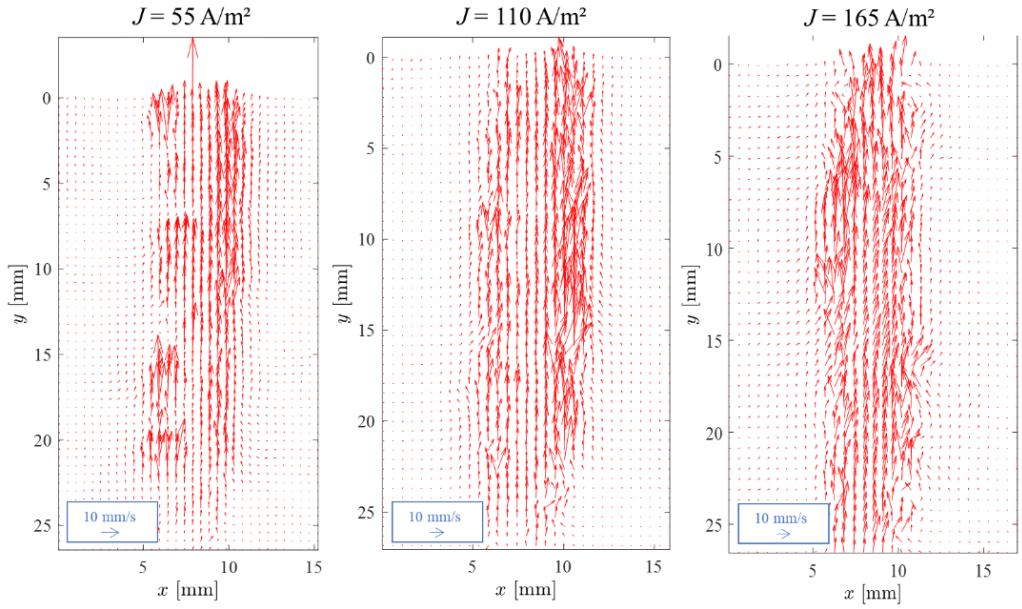

Figure 5. Samples of velocity fields obtained from the optical flow method for 30% KOH.

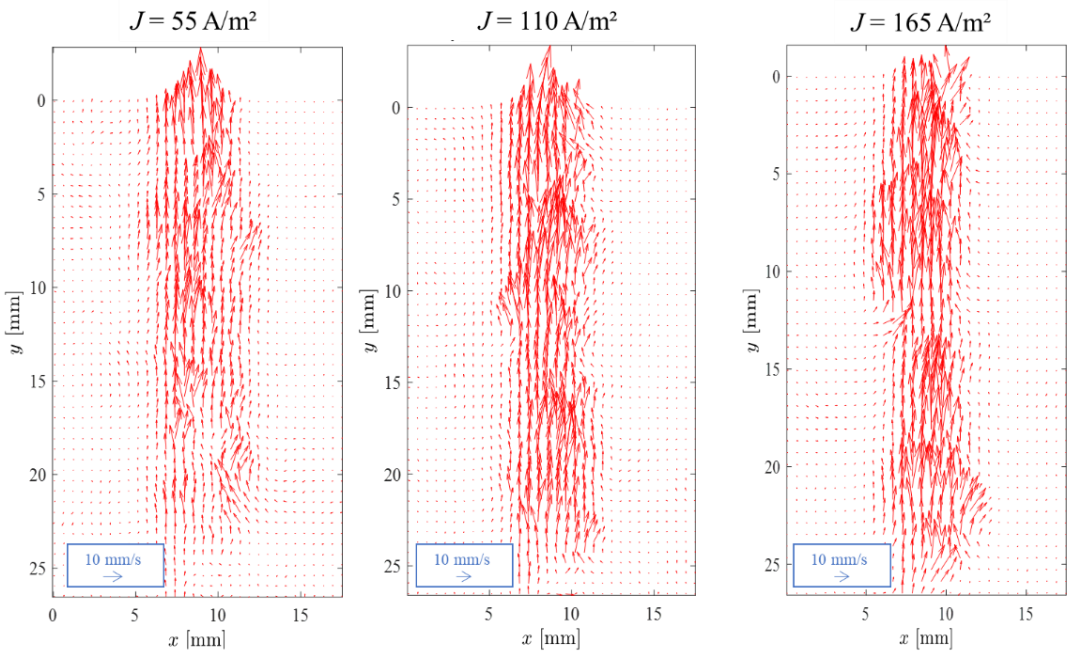

Figure 6. Samples of velocity fields obtained from the optical flow method for 30% KOH with IL.

In Fig. 7, the y-component of velocity (u_y) is depicted for various depth levels relative to the electrode surface. Notably, peaks of maximum velocity rise with increased current density; however, these peaks occur at varying depths. This phenomenon arises from creating circulation structures at different vertical positions between the electrodes.
For the cases of J = 55 and 110 A/m², for example, the highest speed peak is observed at a depth of -4 mm. This is due to the bubbles experiencing vertical acceleration along the electrode. However, this acceleration decreases between depths of -4 mm and -8 mm, causing the speed peaks to diminish at shallower depths. For the case of J = 165 A/m², the speed peaks are observed at greater depths (0 and 4 mm). This indicates that increasing the current density leads to higher speed peaks at greater depths. In all three cases, the vertical speed profile shows irregular behavior due to varying speeds at each depth.

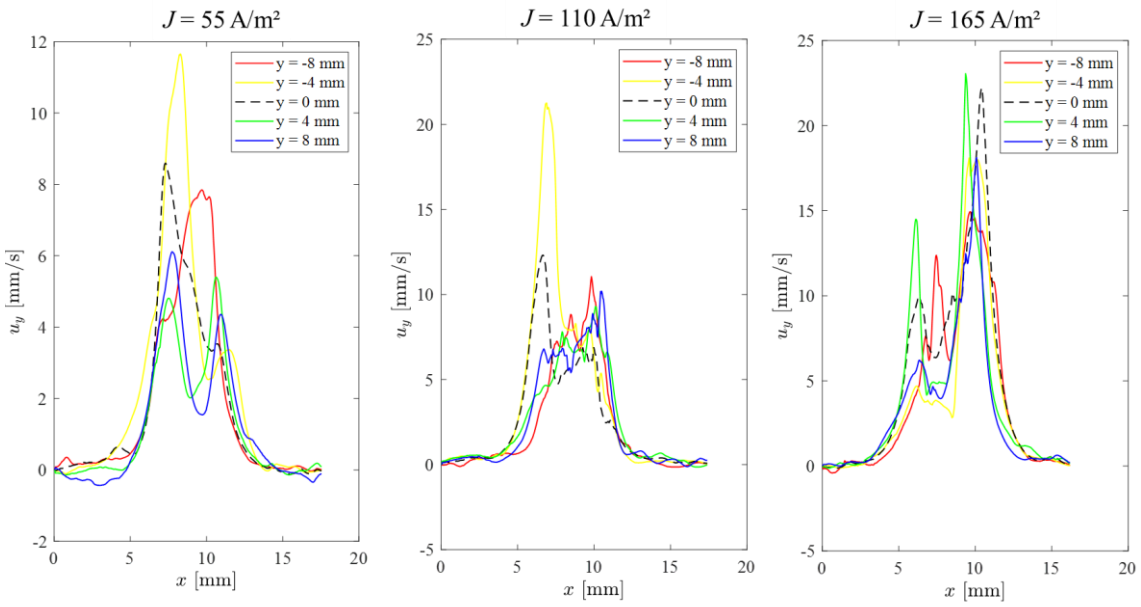

Figure 7. Vertical velocity component for different depth levels from the electrode surface for 30% KOH.

In addition to increasing the conductivity of the medium, the presence of the IL in the electrolyte alters the vertical velocity profile of the bubbles, as shown in Figure 8, for the cases of J = 110 and 165 A/m². This is due to the

increased bubble generation rate, which causes the bubbles to be released at shorter time intervals. The decrease in the thickness of the bubble curtain, as previously mentioned, also contributes to the stability of the vertical velocity profile.

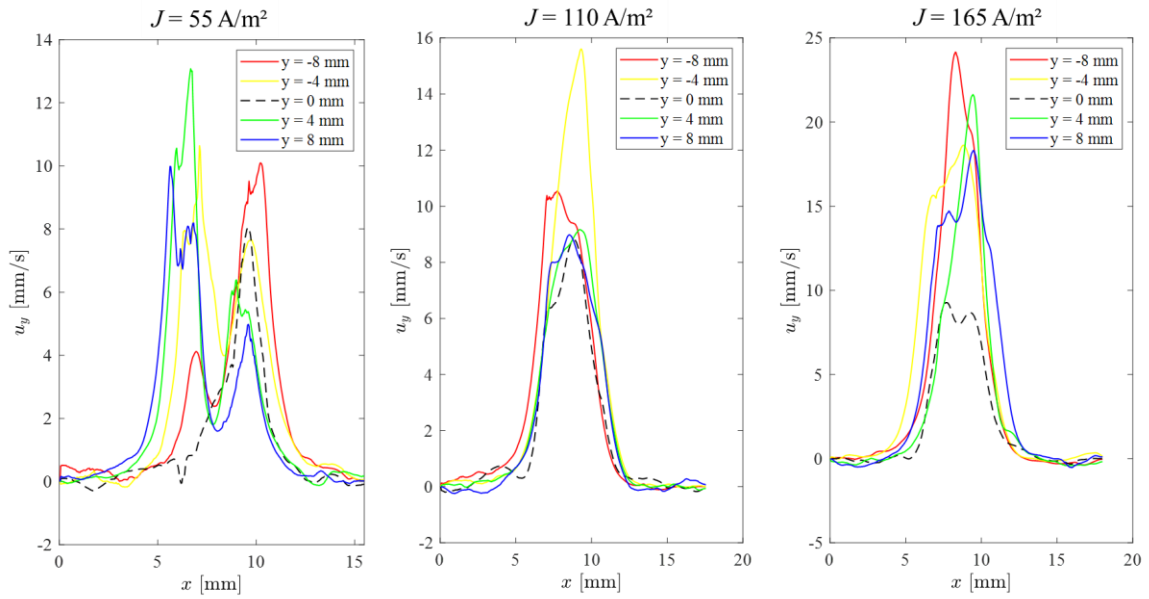

Figure 8. Vertical velocity component for different depth levels from the electrode surface for 30% KOH with IL.

Figure 9 presents samples of vorticity fields for different current densities with and without IL. In the case of the electrolyte with only KOH, the increase in current density increases the presence of vortices near the electrode. On the other hand, in the case of KOH+IL, the increase in current density decreases the presence of vortices, reducing the presence of turbulence during the bubble dynamics. However, in all cases, the greatest intensity of vorticity is observed in the upper region of the electrode.

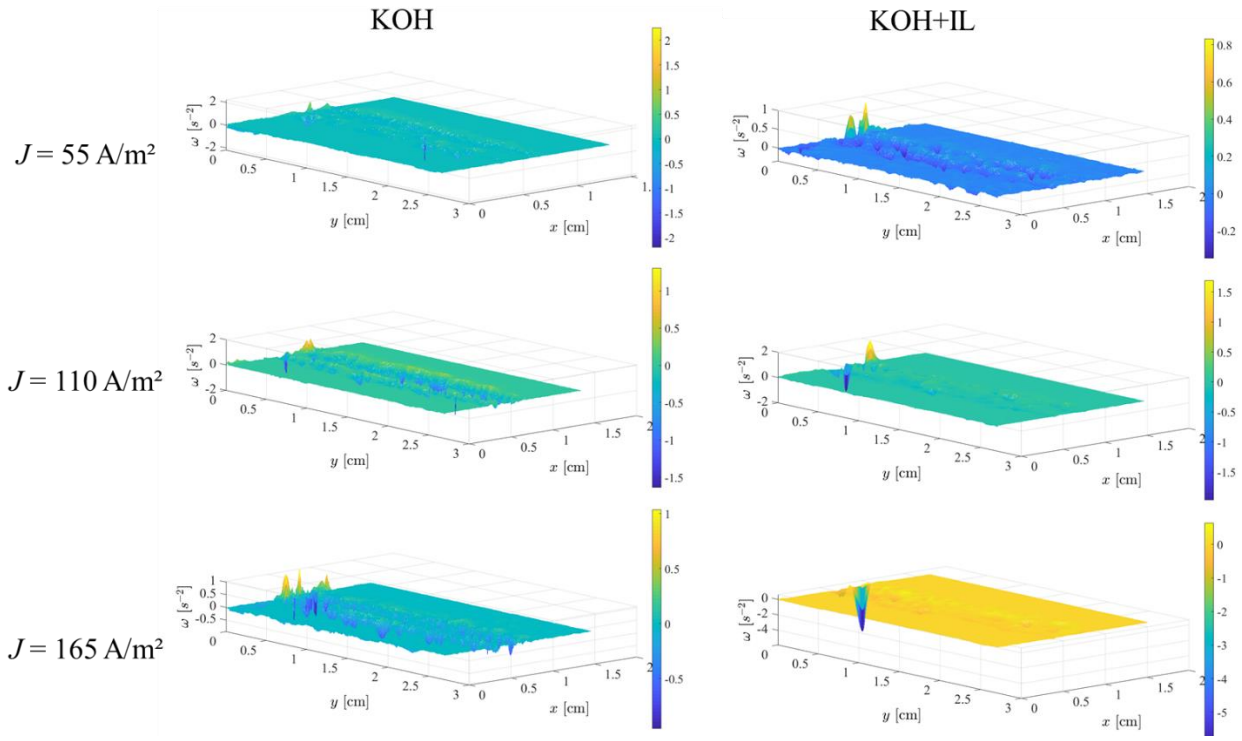

Figure 9. Samples of vorticity fields.

4. CONCLUSION

This study explored bubble dynamics and velocity fields in alkaline water electrolysis, focusing on the effects of current density and ionic liquid (IL) addition. Findings reveal that increasing current density intensifies bubble formation and turbulence, leading to more erratic velocity profiles. The inclusion of IL improves electrolyte conductivity, stabilizing the velocity profile and reducing turbulence. This indicates that IL can enhance electrolysis efficiency by promoting more controlled bubble dynamics. Overall, these insights are valuable for optimizing electrolysis systems and advancing sustainable hydrogen production. Further research could investigate additional electrolyte compositions and configurations to improve efficiency and stability.

5. ACKNOWLEDGEMENTS

We gratefully acknowledge the support of the RCGI – Research Centre for Greenhouse Gas Innovation (Cod. ANP 23.697-6/Cod. FUSP 403904), hosted by the University of São Paulo (USP) and sponsored by FUSP – University of São Paulo and Petronas, as well as the strategic importance of the support given by ANP (Brazil's National Oil, Natural Gas and Biofuels Agency) through the R&DI levy regulation.

6. REFERENCES

Abdelouahed, L., Hreiz, R., Poncin, S., Valentin, G., Lapicque, F., 2014. "Hydrodynamics of gas bubbles in the gap of lantern blade electrodes without forced flow of electrolyte: experiments and CFD modelling". *Chem. Eng. Sci.* 111:255–265.

Avci, AC., Toklu, E., 2022. “A new analysis of two phase flow on hydrogen production from water electrolysis”. *Int. J. Hydrogen Energy* 47(11):6986–95.

Borba, K.N., Trombetta, F., Souza, R.F., Martini, E.M.A., 2017. "Stability of Al2O3/Al in ionic liquid BMI.BF4/γ-butyrolactone electrolytes for use in electrolytic capacitors". *Ionics* 23:1165–1171.

Chandran, P., Bakshi, S., Chatterjee, D., 2015.“Study on the characteristics of hydrogen bubble formation and its transport during electrolysis of water”. *Chem. Eng. Sci.*138:99–109.

Chen, Q., Lin, W., Wang, Z., Yu, J., Li, J., Wang, Z., 2022. "Flow field characterization between vertical plate electrodes in a benchscale cell of electrochemical water softening". *Water Sci. Technol*. 85:1736–1753.

Chien, F.S., Ngo, Q.T., Hsu, C.C. et al., 2021. "Assessing the capacity of renewable power production for green energy system: a way forward towards zero carbon electrification". *Environ. Sci. Pollut. Res.* 28:65960–65973.

Dupont, J., Eberlin, N.M., Consortis, S.C., Santos, S.L., 2006. "The role of ionic liquids in co-catalysis of Baylis-Hillman reaction: interception of supramolecular species via electrospray ionization mass spectrometry". *J. Phys. Org. Chem*. 19:731–736.

Horn, B.K., Schunck, B.G., 1981. "Determining optical flow". *Artif. Intell.* 17:185–204.

Jianu, O.A., Rosen, M.A., Naterer, G.F., Wang, Z., 2015. “Two-phase bubble flow and convective mass transfer in water splitting processes”. *Int. J. Hydrogen Energy* 40:4047–55.

Li, R., Tan, R., Cheong, L., 2017. "Robust optical flow estimation in rainy scenes". *Proc. Eur. Conf. Comput. Vis.* 17:288–304.

Li, Y., Yang, G., Yu, S., Mo, J., Li, K., Xie, Z., Ding, L., Wang, W., Zhang, F-Y., 2021. “High-speed characterization of two-phase flow and bubble dynamics in titanium felt porous media for hydrogen production”. Electrochim. Acta 370:137751.

Liu, T., Shen, L., 2008. "Fluid flow and optical flow". *J. Fluid Mech.* 614:253–291.

Loget, G., Padilha, C.J., Martini, A.E., Souza, O.M., Souza, F.R., 2009. "Efficiency and stability of transition metal electrocatalysts for the hydrogen evolution reaction using ionic liquids as electrolytes". *Int. J. Hydrog. Energy* 34:84–90.

Mei, L., Lai, J., Xie, X., Zhu, J., Chen, J., 2019. "Illumination-invariance optical flow estimation using weighted regularization transform". *IEEE Trans. Circuits Syst. Video Technol.* 30:495–508.

Nasser, M., Megahed, T.F., Ookawara, S. et al., 2022. "A review of water electrolysis–based systems for hydrogen production using hybrid/solar/wind energy systems". *Environ. Sci. Pollut. Res*. 29:86994–87018.

Oliveira, J.D., Cardoso, E.M., Souza, R.R., Copetti, J.B., Varón, L.M., Moreira, J.R.S., 2024. “On fluctuations in velocity fields during convective mass transfer in hydrogen generation through water electrolysis”. Int. J. Hydrogen Energy 80:394–405.

Park H-K, Han J-W, Chung B-J., 2022. “Influence of hydrodynamic parameters on the critical current density at water electrolysis: mass flux, channel inclination and inlet void fraction”. *Int. J. Hydrogen Energy* 47(12):7535–46.

Souza, F.R., Padilha, C.J., Gonçalves, S.R., Dupont, J., 2003. "Room temperature dialkylimidazolium ionic liquid-based fuel cells". *Electrochem. Commun.* 5:728–731.

Souza, F.R., Loget, G., Padilha, C.J., Martini, A.E., Souza, O.M., 2009. "Molybdenum electrodes for hydrogen production by water electrolysis using ionic liquid electrolytes". *Electrochem. Commun.* 10:1673–1675.

Sun, D., Roth, S., Black, M.J., 2014. "A quantitative analysis of current practices in optical flow estimation and the principles behind them". *Int. J. Comput. Vis.* 106:115–137

Trombetta, F., Souza, O.M., Souza, F.R., Martini, A.M., 2019. "Electrochemical behavior of aluminum in 1-n-butyl-3-methylimidazolium tetrafluoroborate ionic liquid electrolytes for capacitor applications". *J. Appl. Electrochem.* 39:2315–2321.

Vogt, H. "Heat transfer in boiling and mass transfer in gas evolution at electrodes-The analogy and its limits". *Int. J. Heat Mass Trans*. 2013, 59:191–197.

Zhang, C., Chen, Z., Wang, M., Li, M., Jiang, S., 2017. "Robust nonlocal optical flow estimation with occlusion detection". *IEEE Trans. Image Process.* 26:4055–4067

Zhen, C., Ge, L., Chen, Z., Li, M., Liu, W. and Chen, H., 2020. "Refined TV-L optical flow estimation using joint filtering". *IEEE Trans Multimedia* 22:349–364

Zhu, J., Zhang, X., Lv., P., Wang Y, Wang J. 2018. “An experimental investigation of convective mass transfer characterization in two configurations of electrolyzers”. *Int. J. Hydrogen Energy* 43(18):8632–43

7. RESPONSIBILITY NOTICE

The authors are the only ones responsible for the printed material included in this paper.